

NORTHWESTERN UNIVERSITY

Photoluminescence Mechanism in Silicon Nanostructure

A DISSERTATION

SUBMITTED TO THE GRADUATE SCHOOL  
IN PARTIAL FULFILLMENT OF THE REQUIREMENTS

for the degree

Master of Science in Physics

Field of Physics

By

GezahegnAssefa

Science Faculty

March 2007

© Copyright by GezahegnAssefa 2007

All Rights Reserved

# ABSTRACT

Photoluminescence Mechanism in Silicon Nanostructure

GezahegnAssefa

The optical properties of bulk Silicon are deeply modified if the material is manipulated at the nano metric size. In particular the growth of nanocrystalline Silicon(nc-Si) structures constitutes today a promising approach for the development of Silicon based light emitting devices. In this thesis the influence of quantum confinement on the optical properties of nc-Si is investigated. We basically concentrate on the Photoluminescence (PL) of nc-Si. One of the fundamental parameters describing The PL mechanism of nc-Si is the radiative recombination rate. In order to examine the mechanism of the PL from the nc-Si the optical transition and the radiative transition rate are studied based on the quantum confinement(QC)model. We find that the radiative recombination rate varies as  $d^{3-\beta}$ . Where  $d^{3-\beta}$  is the diameter of the spherical crystallites. This result shows that the radiative recombination rate increases with decreasing the size of the nc-Si. As a result, the PL emission intensity enhanced due to QCE and the PL can be tuned into the visible range.

## **Acknowledgements**

I would like to thank my advisor and instructor Dr. S.K. Ghoshal for his support and guidance throughout my graduate study and during the course of this thesis. His limitless and invaluable effort in guiding, supervising, encouraging and providing the necessary materials, for the accomplishment of this thesis gives me a great pleasure. It is him gives me courage in doing my graduate thesis in this way.

I extended my gratitude to my families, Ato Daniel Sima and his families for their being always with me and praying to God for my success. I would like to express my deepest thank to my friend Sisay Zeleke for his help in reading, commenting and providing me a computer facilities in his home.

I am indebted to my friends Gizat Chekol, Gebeyehu Taddesse, Urga Dinegde, Ermias Atnafu, Fufa Sorie, Solomon Abera, Shegaw and others, with whom I have shared and discussed ideason the subject matter as well as on our personal affaires during our stay in the university.

It is my great pleasure to thank Addis Ababa University in offering a scholarship to join the postgraduate program. I would also like to thank the department of Physics for all co-operation I got during my M.Sc studies.

Finally, I would like to extend my appreciation to Shimelis Habte Secondary school teachers especially for physics department teachers and administrators for their kind cooperation during my course graduate studies

Gezahegn Assefa.

March, 2007

## Contents

ABSTRACT	iii
Acknowledgements	iv
List of Figures	vii
Chapter 1. Introduction	1
1.1. Application of Silicon Based Materials	1
1.2. Methods of Fabrication of Nanosilicon	3
1.3. Optical Properties of Silicon Nanocrystals	4
1.4. Thesis Outline	11
Chapter 2. The Pseudopotential Method	12
Chapter 3. Optical Transition and Radiative Recombination Rate	23
3.1. Model of Optical Transition	23
3.2. Radiative Recombination Rate	26
Chapter 4. Results and Discussion	32
Chapter 5. Summary and Conclusions	37
References	39

## List of Figures

## CHAPTER 1

### Introduction

#### 1.1. Application of Silicon Based Materials

Silicon is the dominant semiconductor in the device technology today. There are some reasons why Si is the semiconductor material of choice. Among these the two fundamental reasons are the following. The first is the raw material that can be used to produce Si-wafer (sand) is readily available. The second reason is that it possesses good mechanical and thermal properties. The bulk of the Si-wafer is, for example, provides good mechanical support for the fabricated electronic devices, which reside in the region near the wafer's surface. An alternate material that has been suggested for some time is Gallium Arsenide (GaAs). However, the lack of a native oxide, high processing cost and environmental concerns discourage the industry from implementing GaAs as a feasible solution.

From the native oxide of Si ( $\text{SiO}_2$ ), it is possible to fabricate metal oxide semiconductor field effect transistors (MOSFETs). MOSFETs, are building blocks of that makes up complimentary metal oxide semiconductors (CMOS) circuits. With CMOS technology it is possible to integrate millions of transistors on one chip. These are known as ultra large-scale integrated (ULSI) circuits. Using Si-based

ULSI technology, the semiconductor industry has greatly improved the ability to store, process and communicate information.

Nowadays, the semiconductor industries are working to reduce the cost per function on a chip. There are few methods to do this. Among these methods reducing the size of the device with out affecting the efficiency or with better efficiency (i.e. device scaling) takes the great emphasis.

A variety of Si-based devices were studied, including bipolar transistors [1]. Recent studies suggests that circuit fabricated in CMOS technology are capable of fulfilling application requirements for RF analog in 1-5 GHz range and for high-speed digital circuits at or above the 10Gb/s range and higher reliability when compared to their counter parts [2].

Silicon nanotechnology is up coming and the promising one [3-4]. The Nanosilicon (crystalline as well as amorphous) does luminescence. It is this photoluminescence (PL) properties of nanocrystalline silicon (nc-Si) is of major debates in recent days .

In general, several applications have been predicted for nanocrystals, ranging from simple dyes to magnetic-resonance-imaging contrast agents [5], components of electronic circuits [6], and magnetic media [7], in gradients in catalysts and sensors and so on. All the above applications seek to exploit the tunability provided by the size dependent properties of the nanocrystals [8].

## 1.2. Methods of Fabrication of Nanosilicon

Considering the importance of nanocrystallinities in technological applications, a large number of synthesis methods have evolved in recent years [9,10]. Among the various ways have been used to form low dimensional silicon, we explore three of the approaches.

### 1.2.1. Direct Synthesis of Silicon Clusters

Silicon nanoclusters can be directly synthesized by chemical reaction of suitable reactants, such as pyrolysis of  $Si_2H_6$ , formation of nc-Si by laser induced plasma in  $Si_2H_4$ , combustion of  $SiH_4$ , gas evaporation of silicon [9]. The end product is a suspension of nc-Si in a solvent usually is ethanol.

### 1.2.2. Nanosilicon Produced by Phase Separation.

This method is the most widely used. Various techniques have been employed in this technique. Ion implantation, Low pressure chemical vapour deposition (LP-CVD), and Sputtering, produces nc-Si in a  $SiO_2$  matrix [9]. The difference among them are related to the degree of purity of the film. The purity of nc-Si produced by ion implantation is better than the other techniques.

### 1.2.3. Electrochemical Etching of Silicon

Porous Silicon (P-Si) is obtained by the electrochemical etching of crystalline silicon (C-Si) in Hydrofluoric Acid (HF) rich electrolyte [10]. Following the partial

wafer dissolution, a porous silicon structure is formed where the silicon skeleton is either by interconnected nc-Si or by thin silicon wires. The etching process is self regulated. Once the porous layer formed no further etching of porous layer occurs. The reason for this is the depletion of holes in the etched region of the samples. The anodic current has to be less than the electro-polishing current, above which electro-polishing of the silicon occurs and the final layer has mirror like nature without any porous silicon in it.

### **1.3. Optical Properties of Silicon Nanocrystals**

Bulk Semiconductors are characterized by fully filled valance band and entirely empty conduction bands, which are separated by a forbidden range of energies. Thus, conduction in such materials requires a finite energy to promote the transition from the valance band to the conduction band. The gap between valance and conduction band is of fundamental importance for the properties of a solid. Most of the solids properties, such as intrinsic conductivity, electronic transitions or optical transitions depend on it. Any change of the gap significantly alters the material's physics and chemistry. Within the framework of band theory of solids, bulk silicon has indirect band gap, i.e., the energy maxima in the valance band and minima in the conduction bands do not occur in the same k point. Because the momentum of a photon is very small compared to the crystal momentum, the optical process should conserve the momentum of the electron. In a direct transition,

momentum conservation involves states having the same k-values.

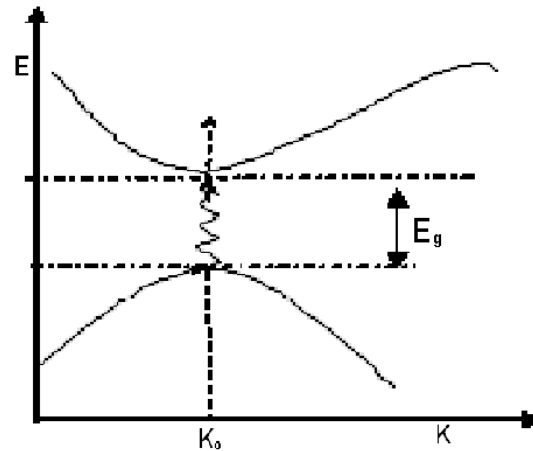


*Fig 1.1a. Direct transition between valance band conduction bands*

In an indirect gap semiconductor momentum is conserved via a phonon interaction. Although broad spectrum of phonons is available, only those phonons with the required momentum change are functional. These are usually the longitudinal and transverse acoustic phonons. So the indirect process is a two step event. Therefore, indirect optical transitions have very low transition probabilities. In addition, bulk crystalline silicon is a centro-symmetric crystal that does not show PL. i.e., it emits light in the infrared region and at a very low efficiency (one photon emitted for every  $10^7$  photo generated electron-hole pair) [11,12].

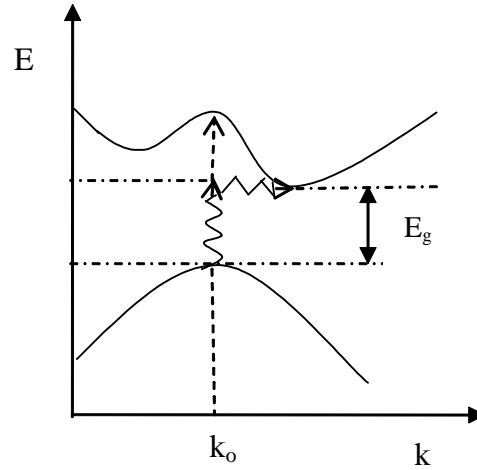


*Figure.1.1b. Indirect transition between valance band and conduction band.*

The situation shown in fig- 1.1b is an indirect transition between the valance band maxima and conduction band minima for which  $\hbar\omega = E_c(k) - E_v(k) \pm \omega_p$ , where  $\omega_p$  is the frequency of the relevant phonon that determines the onset of optical transition.

In semiconductors the absorption of a photon causes the valance band electrons to be promoted into the conduction band, leaving holes behind in the valance band. The de-excitation of electrons by making a transition from the bottom of the conduction to the top of the valance band is a band gap recombination. The electron-hole bound pairs created during the recombination process are known as excitons [13]. When an electron-hole pair is created by absorption of photon, the absorption spectrum contains sharp lines just below the band gap energy. The

lines are due to exciton levels. Excitonic recombination is an important feature of PL. Optical absorption in semiconductor nanocrystals is different form that of the bulk system. They show much change in their electronic properties down to a very small size, about 10nm and below [14]. The origin of such alteration of electronic properties is however still not clear.

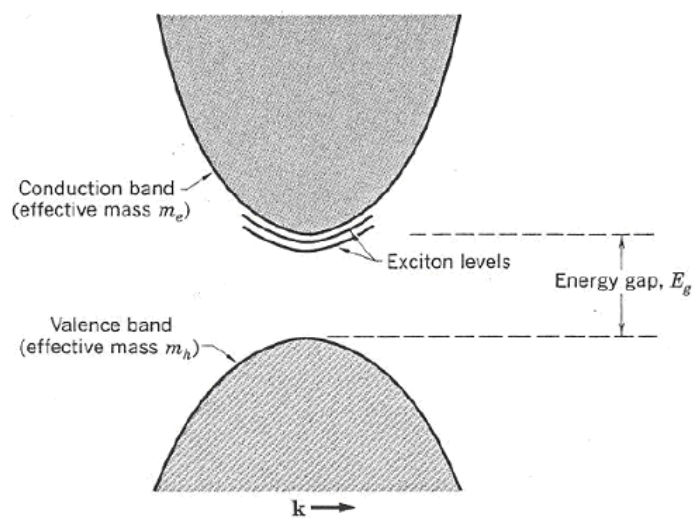


*Figure.1.2. Schematic diagram of exciton levels in semiconductors*

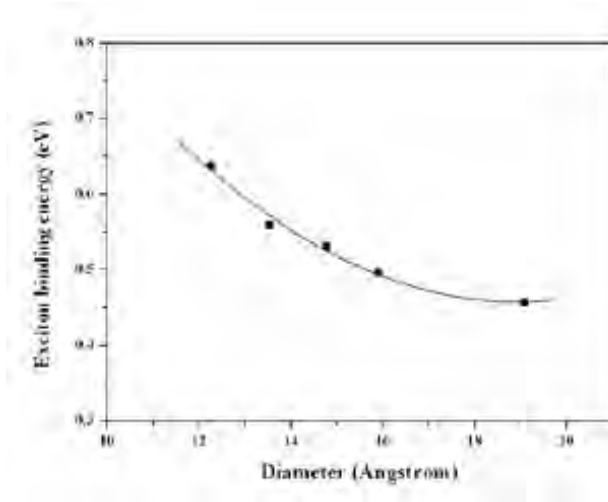


*Figure 1.3 Variation of the exciton binding energy with size*

There has been a great increase in research in the field of nanocrystals during the past decades. Even though research on nanocrystals started in the early eighties, a radical progress was observed in the nineties with emergence of improved techniques for the synthesis of high quality nanocrystals and better instruments to characterize them. Also, the growing need to reduce the size of the integrated circuit chips gave the field of nanotechnology a great emphasis [15].

The band gap of bulk silicon ( $\simeq 1.12eV$ ) is ideal for room temperature operations; however, the discovery of visible PL at room temperature from porous silicon (P-Si) [16] has generated much attention in nanocrystalline silicon (nc-Si) because of the possibility of wide application in opto-electronic devices [12]. When this idea is realized, device science will mark a new progress since silicon is a dominant material in the present day microelectronics technology.

Recent evidences from the experimental researches has shown that accompanying the reduction in size of nc-Si , the band transforms from indirect to direct and the band gap energy is blue shifted into the range of visible light owing to the quantum confinement effect (QCE) [11,12]. Understanding the role of QCE in altering optical properties of semiconductor materials with reduced dimensions is a problem of both the technological and fundamental interest. There is a great deal of experimental and theoretical evidences that supports the important role played by QCE, in producing PL [15]. Excitations in confined system, like silicon quantum dots (Si-QDs), as a building block of nano sized silicon, differ from the bulk system due to QCE. In particular, the components that comprise the exciton energies such as quasi-particle and exciton binding energies change significantly with the physical extent of the system.

The electron-hole exchange interaction can be considered as a very weak perturbation in bulk semiconductors. It is only weakly modifies the structure and energy of the exciton. For instance for exciton in the bulk silicon the exchange splitting energy is about 150 eV [17] and does not play any role in the optical transitions. Its value is proportional to the spatial overlap between the electron and holes. In quantum dots the spatial overlap is increased and the exchange correlation of the coulomb energy is larger when the size of the crystallites approaches to the bulk exciton radius and has to expect a drastic change of the effect. Recently it has been noticed that the electron-hole exchange interaction play a vital role in the description of the basic optical properties of nonocrystalline assemblies [18].

The characteristics of the PL are changed as the wavelength of emission [19] changes from ultraviolet wavelengths to infrared wavelength. A specific characteristic normally applies to a discrete set of wavelength and has resulted in a grouping of wavelengths into three bands to describe these characteristics. These are the ‘red’, ‘blue’, and ‘infrared’ bands. The PL of the blue bands is obtained when the sample contains a large amount of oxygen [18], which has been achieved by oxidation, rapid thermal oxidation.

Nanocrystal quantum dots (NCQDs) are chemically synthesized semi-conducting particles that show discrete atomic-like electronic level structure and optical transition. NCQDs usually consists of a crystalline semiconductor core, often no longer than just a few nanometers in diameter and a surrounding shell. The shell provides the confining effect for the core electrons. They are building blocks for a range of photonic applications. Their absorption and emission wavelengths can be tuned by controlling their size as well as their constituent materials. Recently, efforts have been made to design NCQDs that emit light in the near infrared spectral range [20] due to their importance in optical networking applications and many other optoelectronic uses.

The mechanism responsible for nanosilicon light emission is the matter of great controversy; however, there are different models to explain its luminescence. Basically they can be grouped into three categories. These are the quantum recombination model, the surface state model, and the molecular recombination model [21].

The first two models rely on the QCE. Where as the third model is based on the molecular species such as polysillane chains or siloxen rings present in the nanosilicon (amorphous phase) and are responsible for PL [11].

Different theoretical and experimental works has been done in order to explain the size dependent properties of semiconductor nanocrystals. These works are primarily based on the Effective Mass approximation (EMA) method [22], Empirical Pseudopotential Approach (EPA)[23], and Tight-Binding Scheme [24].

#### 1.4. Thesis Outline

In this thesis we study the optical transition between the HOMO-LUMO states of silicon nanocrystal. For this study the PL is considered due to the radiative recombination of photo-carriers due to the QCE (quantum recombination model). The thesis is organized into five chapters. Chapter 2 discusses the pseudopotential calculation for the Hamiltonian of Ns-QDs'. Chapter 3 discusses how the radiative recombination rate is related to the size of the QD. We use the empirical pseudopotential approach to calculate the Hamiltonian and the optical transition probabilities of silicon nanocrystal. Because in our calculation the wavefunctions of the nc-si can be composed of energy band states of the bulk, the HOMO and the LUMO states, and by assuming that the electronic properties are mostly rely on the valence electrons rather than the core electrons. Chapter 4 contains the result and discussion, and chapter 5 gives the summary and conclusion.

## CHAPTER 2

### **The Pseudopotential Method**

In this chapter we present the form of pseudopotential required for the electronic band structure calculations of Silicon quantum dots.

On the microscopic scale, solid state materials are made up of a crystal lattice of atoms. The crystal lattice is a highly ordered system that is composed of a repeating pattern of atoms. Because there is a potential energy associated with each atom, it follows that an electron in the crystal lattice will experience a periodic potential due to the repetition of atoms in the crystal. Quantum mechanics predicts that a finite number of states are available to an electron in the lattice. The finite state comes from finite number of energy levels associated with each atom in the crystal. To make calculations regarding macroscopic properties of solids, it is often necessary to understand the potential that an electron felt in the periodic lattice.

Assuming that the inner electrons (core electrons), screen the outer valence electrons from the central nuclear charge and they are tightly bound to the nucleus, the effective potential by an electron in a crystal is weak compared with coulomb potential of the ion core. We also assume that the nucleus passes no energy to the electrons, which then allows the decoupling of the motion of the nuclei and electrons motions. The core electrons are treated as if they were frozen in atomic

like configuration. As a result, the valence electrons are thought to move in a weak one-electron potential called pseudopotential.

The pseudopotential method is introduced to explain why the effective potential on an electron in a crystal is weak as compared with the coulomb potential of the ion core. Since the pseudopotential is an extension of orthogonalized plane wave (OPW) method, it requires that the free electron wave function  $\psi_{\mathbf{k}}$  be orthogonal to the atomic core state. According to the orthogonality requirement there exist a Bloch function  $\varphi_{\mathbf{k}}$  which is orthogonal to the atomic core function  $\phi_{\mathbf{k}}$ , and which looks like  $\varphi_{\mathbf{k}}$  as well as having some components of core state is expressed as

$$\psi_{\mathbf{k}} = \varphi_{\mathbf{k}} + \sum_{\alpha} b_{\alpha} \phi_{\mathbf{k},\alpha} \quad (2.1)$$

Where  $\phi_{\mathbf{k}}$  is a normalization core state,  $b_{\alpha}$  are orthogonalization coefficients. The sum is taken over all atomic core states. For silicon the summation over  $\alpha$  is a sum over all core state  $1s^2 2s^2 2p^6$ . The constants are determined using the fact that the crystal wave function is constructed to be orthogonal to the core wave function. We have,

$$\int \phi_{\mathbf{k},\alpha}^* \psi_{\mathbf{k}} d\mathbf{r} = 0, \quad (2.2)$$

$$b_{\alpha} = - \int \phi_{\mathbf{k},\alpha}^* \varphi_{\mathbf{k}} d\mathbf{r}, \quad (2.3)$$

$$\psi_{\mathbf{k}} = \varphi_{\mathbf{k}} - \sum_{\alpha} \left( \int \phi_{\mathbf{k},\alpha}^* \varphi_{\mathbf{k}} d\mathbf{r} \right) \phi_{\mathbf{k},\alpha}. \quad (2.4)$$

Since  $\psi_{\mathbf{k}}$  is an exact valance wave function it satisfy Schrödinger's equation with eigenvalue  $\varepsilon_v$  (valance state energy).

$$\mathbf{H}\psi_{\mathbf{k}} = \varepsilon_v \psi_{\mathbf{k}} \quad (2.5)$$

$$\mathbf{H} \left( \varphi_{\mathbf{k}} - \sum_{\alpha} \left( \int \phi_{\mathbf{k},\alpha}^* \varphi_{\mathbf{k}} d\mathbf{r} \right) \phi_{\mathbf{k},\alpha} \right) = \varepsilon_v \left( \varphi_{\mathbf{k}} - \sum_{\alpha} \left( \int \phi_{\mathbf{k},\alpha}^* \varphi_{\mathbf{k}} d\mathbf{r} \right) \phi_{\mathbf{k},\alpha} \right) \quad (2.6)$$

$$\mathbf{H}\varphi_{\mathbf{k}} - \sum_{\alpha} \left( \int \phi_{\mathbf{k},\alpha}^* \varphi_{\mathbf{k}} d\mathbf{r} \right) \mathbf{H}\phi_{\mathbf{k},\alpha} = \varepsilon_v \varphi_{\mathbf{k}} - \sum_{\alpha} \left( \int \phi_{\mathbf{k},\alpha}^* \varphi_{\mathbf{k}} d\mathbf{r} \right) \varepsilon_v \phi_{\mathbf{k},\alpha} \quad (2.7)$$

For exact core level,  $\mathbf{H}\phi_{\mathbf{k},\alpha} = \varepsilon_c \phi_{\mathbf{k},\alpha}$

$$\mathbf{H}\varphi_{\mathbf{k}} + (\varepsilon_v - \varepsilon_c) \sum_{\alpha} \left( \int \phi_{\mathbf{k},\alpha}^* \varphi_{\mathbf{k}} d\mathbf{r} \right) \phi_{\mathbf{k},\alpha} = \varepsilon_v \varphi_{\mathbf{k}}. \quad (2.8)$$

Defining a new potential  $V_{\mathbf{R}}$  as

$$V_{\mathbf{R}} = \frac{(\varepsilon_v - \varepsilon_c) \sum_{\alpha} \left( \int \phi_{\mathbf{k},\alpha}^* \varphi_{\mathbf{k}} d\mathbf{r} \right) \phi_{\mathbf{k},\alpha}}{\varphi_{\mathbf{k}}}, \quad (2.9)$$

$V_{\mathbf{R}}$  represents a short range, non-Hermitian repulsive potential.

Equation (2.8) can be written as

$$(\mathbf{H} + V_{\mathbf{R}}) \varphi_{\mathbf{k}} = \varepsilon_v \varphi_{\mathbf{k}}. \quad (2.10)$$

Equation (2.10) can be thought as a wave function of the pseudo-wave function  $\varphi_{\mathbf{k}}$ , with energy eigenvalue of the true energy of the crystal wave function  $\psi_{\mathbf{k}}$ . Due to the orthogonalization requirement, the repulsive potential  $V_{\mathbf{R}}$  provides a partial cancellation of the attractive periodic potential, and leads to a potential weak enough to do nearly free description. The pseudopotential ( $V_p$ ) is then the sum of the actual periodic potential  $V_c$  and  $V_{\mathbf{R}}$ .

$$V_p = V_c + V_{\mathbf{R}} \quad (2.11)$$

For silicon atom of electronic configuration  $1s^2 2s^2 2p^6 3s^2 3p^6$  the core consists of four s-state electrons and six p-state electrons. The core electrons of s-states have much lower energy than the valence electrons; as a result  $V_c$  and  $V_{\mathbf{R}}$  nearly cancel each other. Where as the core p-state pushes the valence electrons away from the core due to their large energy, i.e., there exists less cancellation of  $V_c$  and  $V_{\mathbf{R}}$  terms. In general the smoothly varying pseudopotential is sufficient to describe the electronic structure of a complicated multidimensional physical system using the nearly free electron model.

From the result obtained in equation (2.11) the self interacting electron clouds within the plasma of the crystal can be simplified in to one-electron problem with the following Hamiltonian.

$$\mathbf{H} = -\frac{\hbar^2 \nabla^2}{2m} + V_p, \quad (2.12)$$

$$\mathbf{H}\varphi_{n,\mathbf{k}} = E_{n,\mathbf{k}}\varphi_{n,\mathbf{k}}. \quad (2.13)$$

The solution to the Schrödinger Wave equation in a periodic lattice is a Bloch function which is composed of a plane wave component as well as a cell periodic part that has the periodicity of the lattice. The pseudo-wave function (with the  $n^{\text{th}}$  band and the wave vector  $\mathbf{k}$ ) is the wave function of electrons in the periodic lattice, and can be expanded in complete orthogonal sets of plane waves:

$$U_{G,\mathbf{k}} = \frac{1}{\sqrt{\Omega}} e^{i(\mathbf{G}+\mathbf{k})\cdot\mathbf{r}}, \quad (2.14)$$

$$\varphi_{n,\mathbf{k}} = \frac{1}{\sqrt{\Omega}} \sum_{\mathbf{G}} a_{n,\mathbf{k}}(\mathbf{G}) e^{i(\mathbf{G}+\mathbf{k})\cdot\mathbf{r}}. \quad (2.15)$$

Where  $\mathbf{G}$ , is reciprocal lattice vector describing the periodicity of the lattice which satisfies  $\mathbf{G} \cdot \mathbf{R} = 2\pi n$ ,  $n \in \mathbb{Z}$  where  $\mathbf{R}$  is the Bravais lattice vector.

Substituting the expansion of  $\varphi_{n,\mathbf{k}}(\mathbf{r})$  in equation (2.14) in to Schrödinger equation, and utilizing linearity of the Hamiltonian, we obtain,

$$\sum_{\mathbf{G}} a_{n,\mathbf{k}}(\mathbf{G}) \mathbf{H} U_{\mathbf{G},\mathbf{k}} = E_{n,\mathbf{k}} \sum_{\mathbf{G}} a_{n,\mathbf{k}}(\mathbf{G}) U_{\mathbf{G},\mathbf{k}} \quad (2.16)$$

Multiplying equation (2.15) by a particular wave  $U_{\mathbf{G},\mathbf{k}}$  and integrating over all spaces, then

$$\sum_{\mathbf{G}} a_{n,\mathbf{k}}(\mathbf{G}) \int U_{\mathbf{G}',\mathbf{k}}^* \mathbf{H} U_{\mathbf{G},\mathbf{k}} d\mathbf{r} = E_{n,\mathbf{k}} \sum_{\mathbf{G}} a_{n,\mathbf{k}}(\mathbf{G}) \int U_{\mathbf{G}',\mathbf{k}} U_{\mathbf{G},\mathbf{k}}^* d\mathbf{r}. \quad (2.17)$$

Defining a new Hamiltonian  $\mathbf{H}_{\mathbf{G}',\mathbf{G}}$  as  $\mathbf{H}_{\mathbf{G}',\mathbf{G}} = \int U_{\mathbf{G}',\mathbf{k}}^* \mathbf{H} U_{\mathbf{G},\mathbf{k}} d\mathbf{r}$  and using orthogonality of basis sets  $\int U_{\mathbf{G}',\mathbf{k}}^* U_{\mathbf{G},\mathbf{k}} d\mathbf{r} = \delta_{\mathbf{G}',\mathbf{G}}$ , equation (2.16) can be written as:

$$\sum_{\mathbf{G}} a_{n,\mathbf{k}}(\mathbf{G}) H_{\mathbf{G}',\mathbf{G}} = \sum_{\mathbf{G}} a_{n,\mathbf{k}}(\mathbf{G}) E_{n,\mathbf{k}} \delta_{\mathbf{G}',\mathbf{G}}. \quad (2.18)$$

It remains now to find the eigenvalue and eigenfunction of the square matrix  $\mathbf{H}_{\mathbf{G}',\mathbf{G}}$ , because equation (2.17) can exist to for each value of the electron wave vector  $\mathbf{k}$ . Using the form of the plane waves given in equation (2.14)  $H_{\mathbf{G}',\mathbf{G}}$  can be written as:

$$\mathbf{H}_{\mathbf{G}',\mathbf{G}} = \frac{1}{\Omega} \int e^{-i(\mathbf{G}'+\mathbf{k})\cdot\mathbf{r}} \left( \frac{-\hbar}{2m} \nabla^2 \right) e^{i(\mathbf{G}+\mathbf{k})\cdot\mathbf{r}} d\mathbf{r} + \frac{1}{\Omega} \int e^{-i(\mathbf{G}'+\mathbf{k})\cdot\mathbf{r}} V_0 e^{i(\mathbf{G}+\mathbf{k})\cdot\mathbf{r}} d\mathbf{r}, \quad (2.19)$$

$$H_{\mathbf{G}',\mathbf{G}} = \frac{\hbar^2}{2m\Omega} \int |\mathbf{G} + \mathbf{k}|^2 e^{i(\mathbf{G}-\mathbf{G}')\cdot\mathbf{r}} d\mathbf{r} + \frac{1}{\Omega} \int e^{-i(\mathbf{G}'+\mathbf{k})\cdot\mathbf{r}} V_0 e^{i(\mathbf{G}+\mathbf{k})\cdot\mathbf{r}} d\mathbf{r}. \quad (2.20)$$

The first term of equation (2.20) has a value if  $\mathbf{G} = \mathbf{G}'$  and it is equal to the normalization volume introduced earlier. Therefore, the first term can be written using the Kronecker delta and the second term is some form of pseudopotential defined by:

$$V_p = \frac{1}{\Omega} \int e^{-i(\mathbf{G}'+\mathbf{k})\cdot\mathbf{r}} V_0 e^{i(\mathbf{G}'+\mathbf{k})\cdot\mathbf{r}} d\mathbf{r}. \quad (2.21)$$

Therefore,

$$\mathbf{H}_{\mathbf{G}',\mathbf{G}} = \frac{\hbar^2}{2m\Omega} \int |\mathbf{G} + \mathbf{k}|^2 \delta_{\mathbf{G}',\mathbf{G}} + V_p \quad (2.22)$$

The potential  $V_0$  should be the linear combination of atomic potential  $V_a$ , which is located at  $\mathbf{R}$ , i.e.

$$V_0 = \sum_{\mathbf{R}} V_a(\mathbf{r} - \mathbf{R}) \quad (2.23)$$

Substituting equation (2.23) into equation (2.21), we obtain:

$$V_p = \frac{1}{\Omega} \sum_{\mathbf{R}} \int V_a(\mathbf{r} - \mathbf{R}) e^{i(\mathbf{G}-\mathbf{G}')\cdot\mathbf{r}} d\mathbf{r} \quad (2.24)$$

Performing the transformation,  $\mathbf{r} \rightarrow \mathbf{r} + \mathbf{R}$ , then we obtain

$$V_p = \frac{1}{\Omega} \sum_{\mathbf{R}} e^{i(\mathbf{G}-\mathbf{G}')\cdot\mathbf{R}} \int V_a(\mathbf{r}) e^{i(\mathbf{G}-\mathbf{G}')\cdot\mathbf{r}} d\mathbf{r}. \quad (2.25)$$

The term  $\sum_{\mathbf{R}} e^{i(\mathbf{G}-\mathbf{G}')\cdot\mathbf{R}}$  is known as the geometrical structure factor  $S$ . and  $\mathbf{G} - \mathbf{G}' = \mathbf{q}$  is another reciprocal lattice vector, with the property  $\mathbf{R} \cdot \mathbf{q} = 2\pi n$ ,

$n \in z$ . Since the atomic sites are constructed from the Bravais lattice and the basis, then the summation over the atomic site can be replaced by two summations.

$$\sum_{\mathbf{R}} \sum_{\mathbf{T}} e^{i\mathbf{q} \cdot (\mathbf{R} + \mathbf{T})} \quad (2.26)$$

Since for N Bravais lattice in the crystal, equation (2.26) can be written as

$$S(\mathbf{q}) = N \sum_{\mathbf{T}} e^{i\mathbf{q} \cdot \mathbf{T}}. \quad (2.27)$$

Silicon has a face centered cubic Bravais lattice with a two atom basis, hence the summation in equation 2.27 contains two term

$$S(\mathbf{q}) = N (e^{i\mathbf{q} \cdot \mathbf{T}} + e^{-i\mathbf{q} \cdot \mathbf{T}}), \quad (2.28)$$

$$S(\mathbf{q}) = 2N \cos(\mathbf{q} \cdot \mathbf{T}). \quad (2.29)$$

Then the potential  $V_p$  becomes

$$V_p = \frac{2N}{\Omega} \cos(\mathbf{q} \cdot T) \int V_a(\mathbf{r}) e^{i\mathbf{q} \cdot \mathbf{r}} d\mathbf{r}, \quad (2.30)$$

Where  $\int V_a(\mathbf{r}) e^{i\mathbf{q} \cdot \mathbf{r}} d\mathbf{r} = V_{ff}(\mathbf{q})$  is the Fourier transform of atomic potential and is known as pseudopotential form factor. Equation (2.30) can then be written as:

$$V_p = \frac{2N}{\Omega} \cos(\mathbf{q} \cdot \mathbf{T}) V_{ff}(\mathbf{q}). \quad (2.31)$$

Equation (2.31) is a general form of pseudopotential of silicon. This  $q$ -dependent pseudopotential is then used to calculate the energy band structure of silicon along different crystallographic directions. In the next chapter we shall use a Hamiltonian of the form  $\mathbf{H} = -\frac{\hbar^2}{2m} \nabla^2 + V_p(\mathbf{r})$ , where  $V_p(\mathbf{r})$  is the Fourier transform of the pseudopotential described in equation (2.31).

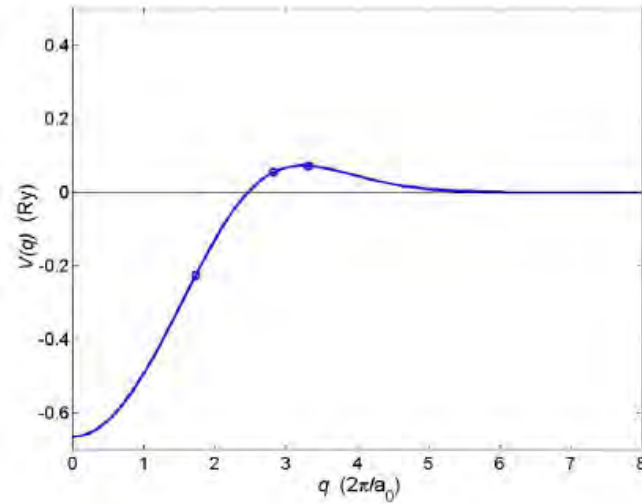
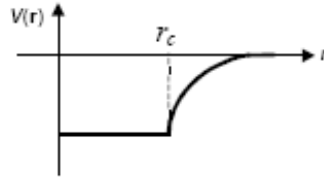


*Fig. 4.1 The Fourier transform of the pseudopotential.*

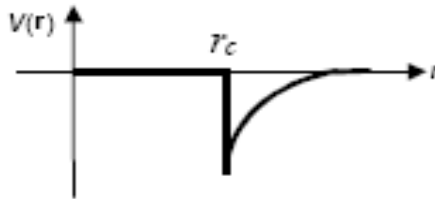
To simplify the problem further, model potentials are used in place of the actual pseudopotentials. Fig.2.2 summarizes the various models those are usually employed.

(a) Constant effective potential in the core region:



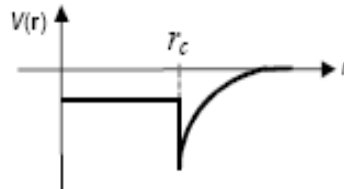
$$V(\mathbf{r}) = \begin{cases} \frac{Ze^2}{4\pi\epsilon_0 r} & : \mathbf{r} > \mathbf{r}_c \\ \frac{Ze^2}{4\pi\epsilon_0 r_c} & : \mathbf{r} \leq \mathbf{r}_c \end{cases}$$

(b) Empty core potential



$$V(\mathbf{r}) = \begin{cases} \frac{-Ze^2}{4\pi\epsilon_0 r} & : \mathbf{r} > \mathbf{r}_c \\ 0 & : \mathbf{r} \leq \mathbf{r}_c \end{cases}$$

(c) Model potential due to Hein and Abarenkov:



$$V(\mathbf{r}) = \left\{ \begin{array}{l} \frac{Ze^2}{4\pi\epsilon_0 r} : \mathbf{r} > \mathbf{r}_c \\ A : \mathbf{r} > \mathbf{r}_c \end{array} \right\}$$

*Fig. 2.2. Model pseudopotentials.*

## CHAPTER 3

### **Optical Transition and Radiative Recombination Rate**

In this chapter we present the theoretical study of optical transition between HOMO- LUMO states of the silicon quantum dots. Since the PL is dependent on the radiative recombination rate of the transition; we discuss how the recombination rate depends on the size of the dot.

#### **3.1. Model of Optical Transition**

The indirect band gap of bulk silicon causes a very long radiative life time (in order of millisecond) for excited electron-hole pairs. Most of the excited electron-hole pairs recombine non-radiatively, giving no luminescence.

In this thesis we focus on the quantum confinement model to explain PL. We considered that the photoemission occurs inside the nc-si particles with energy gap larger than that of the bulk silicon due to QCE. In fact there are long debate concerning the PL mechanism of nc-si, we focus on the role of quantum confinement in the luminescence. For PL from these systems, Qin and Jia [25] suggested a common mechanism model, the so-called the quantum confinement luminescence center (QCLC) model, which claimed that the photoexcitation of electron-hole pairs occurs mainly in the nc-si. The photoexcited electron-hole pairs tunnel into

the luminescence centers (LCs) in the surrounding medium and radiatively recombine there. According to this model, the nc-si particles has recombination center inside the nanocrystal or outside the nanocrystal (inside the surrounding matrix). If the nanocrystal has a recombination center inside, the electron and the hole recombine non-radiatively. These nanocrystals are dark nanocrystals. Bright nanocrystals are those which are free from recombination centers. In these nanocrystals the electron and holes recombine radiatively giving PL.

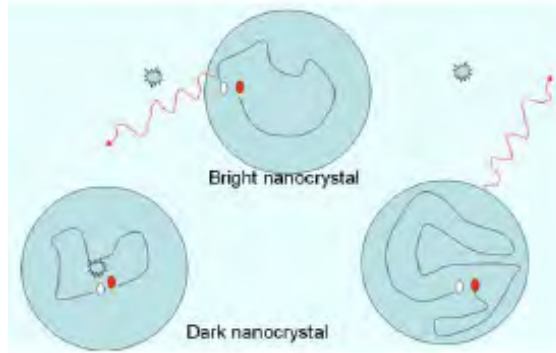


*Figure.3.1 Schematic diagram of nc-si in amorphous matrix. The system in the figure has three electron – hole pairs excited of which one recombine non-radiatively and two radiatively. i.e, the internal quantum efficiency of this system is which is about 67 %.*

Perhaps the most fundamental issue in dealing with nanocrystals is determining their structure. Before any theoretical calculations are performed, the geometry of the nanocrystal must be defined. However, this can be a difficult task. Serious problems arise from the existence of multiple local minima in the potential energy

surface of these system; many similar structures can exist with extremely small energy differences.

In order to formulate and describe the PL phenomena from nc-Si structures, we consider nc-Si as ensemble of nanometric size spherical particles, having a well defined size distribution. The optical band gap widening in the crystallites is considered due to QCE in nanoparticles. We assume that both photo excitation and photo emission processes for electron hole pairs occur in the nanosilicon particles.

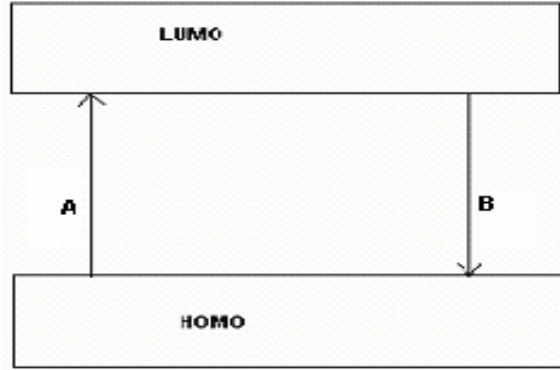


*Fig.3.2. Direct transition between the HOMO and LUMO states during PL emission from nanosilicon crystallites.*

Path A: On excitation with high energy photons, photo carriers are generated in side the crystallites and then relaxed.

Path B: The relaxed carriers recombine to ground states radiatively giving PL.

### 3.2. Radiative Recombination Rate

Optical transition between the lowest unoccupied molecular orbital (LUMO) and the highest occupied molecular orbital (HOMO) is induced due to the illumination of light. Since light is an electromagnetic field (EMF), it is assumed to be of the form

$$E(t) = E(e^{-i\omega t} + e^{i\omega t}) \quad (3.1)$$

The transition between HOMO-LUMO state of  $N$  identical atoms, the wave function of which are the pseudo-wave functions and. The wave functions are then described by Bloch wave functions as

$$\varphi_l(\mathbf{r}) = \frac{1}{\sqrt{\Omega}} e^{i\mathbf{k}\cdot\mathbf{r}} U_l(\mathbf{k}) \quad (3.2)$$

$$\varphi_h(\mathbf{r}) = \frac{1}{\sqrt{\Omega}} e^{i\mathbf{k}'\cdot\mathbf{r}} U_h(\mathbf{k}') \quad (3.3)$$

Where  $\Omega$  refers to the volume element over which the integration is carried out.

The Hamiltonian which describe the interaction of the electromagnetic field with the electronic state is given by

$$\mathbf{H} = \frac{e}{mc} \mathbf{P} \cdot \mathbf{A} \quad (3.4)$$

Where  $\mathbf{P} = -i\hbar\nabla$  is the linear momentum operator and  $\mathbf{A}$  is the vector potential of the electromagnetic field.

Equation (3.4) can be written as

$$\mathbf{H} = -\frac{ie\hbar}{2mc} (\mathbf{A} \cdot \nabla + \nabla \cdot \mathbf{A}) \quad (3.5)$$

The matrix element of the transition is given as

$$\bar{\mathbf{H}}_{hl}(\mathbf{r}) = \int \varphi_h^*(\mathbf{r}) \mathbf{H} \varphi_l(\mathbf{r}) d\mathbf{r} \quad (3.6)$$

By substituting equations (3.2), (3.3), (3.4) into equation (3.6) we obtain

$$\bar{\mathbf{H}}_{hl}(r) = -\frac{ie\hbar}{2mc\Omega} \left[ \int e^{i(\mathbf{k}-\mathbf{k}')\cdot\mathbf{r}} U_h(\mathbf{k}) \mathbf{A} \cdot \nabla U_l(\mathbf{k}) d\mathbf{r} + \int e^{i(\mathbf{k}-\mathbf{k}')\cdot\mathbf{r}} U_h^*(\mathbf{k}') iU_l(\mathbf{k}) \mathbf{A} \cdot \mathbf{k} d\mathbf{r} \right] \quad (3.7)$$

But for direct transitions  $\mathbf{k} = \mathbf{k}'$ , thus we obtain

$$\bar{\mathbf{H}}_{hl}(r) = -\frac{ie\hbar}{2mc\Omega} \left[ U_h^*(\mathbf{k}) \left( \mathbf{A} \cdot \nabla U_l(\mathbf{k}) + iU_l(\mathbf{k}) \mathbf{A} \cdot \mathbf{k} \right) d\mathbf{r} \right] \quad (3.8)$$

The second term of equation (3.7) gives zero since the Bloch functions  $U_h$  and  $U_l$  in the Brillion zone in two different bands is orthogonal. And therefore

$$\bar{\mathbf{H}}_{hl}(r) = -\frac{ie\hbar}{2mc\Omega} \left[ U_h^*(\mathbf{k}) \mathbf{A} \cdot \nabla U_l(\mathbf{k}) d\mathbf{r} \right] \quad (3.9)$$

The momentum operator (some times called the electric dipole transition element) is given as

$$\mathbf{P}_{hl} = -\frac{i\hbar}{\Omega} \int U_h^*(\mathbf{k}) \nabla U_l(\mathbf{k}) dr \quad (3.10)$$

Therefore, equation (3.9) can be rewritten as

$$\bar{\mathbf{H}}_{hl}(r) = \frac{e}{mc} \mathbf{A} \cdot \mathbf{P}_{hl} \quad (3.11)$$

The oscillator strength  $f_{hl}$ , which is the measure of the radiative probability of a quantum mechanical transition between two atomic levels, is related to the momentum matrix element as

$$f_{hl} = \frac{2}{m\hbar\omega_{hl}} |\mathbf{P}_{hl}|^2 \quad (3.12)$$

Where  $\omega_{hl}$  is the frequency of the external EMF with energy equal to the HOMO-LUMO energy gap. The emission and absorption of light by a charged carrier, where an electron or hole is essentially a scattering phenomenon between initial state “h” and final state “l”. The light (EMF) is the time dependent perturbation which induces this event. The transition rate from the initial state to final state is given by the Fermi’s Golden rule as

$$\frac{1}{\tau_{hl}} = \frac{2\pi}{\hbar} \sum_l |\bar{\mathbf{H}}_{hl}|^2 \delta(E_{hl} \pm \hbar\omega) \quad (3.13)$$

Where  $E_{hl} = E_h - E_l$ , which contains both the kinetic and potential energy components. The Delta function now explicitly contains the photon energy with the minus sign representing absorption and the plus sign representing emission.

Substituting equation (3.11) into equation (3.13) we obtain:

$$\frac{1}{\tau_{hl}} = \frac{2\pi e^2 A^2 \cos^2 \theta}{\hbar m^2 c^2} \sum_l |\mathbf{P}_{hl}|^2 \delta(E_{hl} \pm \hbar\omega) \quad (3.14)$$

Equation (3.14) can be written in terms of the oscillator strength in equation (3.12) as:

$$\frac{1}{\tau_{hl}} = \frac{\pi e^2 A^2 \cos^2 \theta}{m c^2} \sum_l f_{hl} \delta(E_{hl} \pm \hbar\omega) \quad (3.15)$$

Considering the continuum limit the total recombination rate can be taken as the integral over the frequency  $d\omega$ .

$$\frac{1}{\tau_{hl}} = \frac{\pi e^2 A^2 \cos^2 \theta}{m c^2} \int \sum_l f_{hl} \delta(E_{hl} \pm \hbar\omega) d\omega \quad (3.16)$$

In the volume there are many states but only those states whose energy difference matched with the frequency of the external EMF would contribute for the transition and for PL. So this would happen for  $E_{hl} = \pm \hbar\omega_{hl}$ . From the property of the delta function, equation (3.16) can be written as

$$\frac{1}{\tau_{hl}} = \frac{\pi e^2 A^2 \cos^2 \theta}{m c^2} \sum_l f_{hl}(\omega_{hl}) \quad (3.17)$$

It is found experimentally that the oscillator strength in the nanocrystallites is dependent on the crystallites size as the inverse power law [26,27]

$$f_{hl} \sim \frac{1}{d^\beta} \quad (3.18)$$

Where  $d$  is the diameter of the spherical crystallites and the power exponent  $\beta$  depends on the material property as well as range of the crystallite size being used, and the value of  $\beta$  is  $5 < \beta < 6$ .

If we assume that each atom in the crystallites contributes at least one photoexcited carrier to the crystallite, the number of photoexcited carriers  $N_p$  in the crystallites is proportional to its volume.

$$N_p \sim \Omega \quad (3.19)$$

For spherical crystallites of diameter  $d$ , the volume  $\Omega$  is proportional to the cube of the diameter

$$\Omega = \frac{4}{3}\pi d^3 \quad (3.20)$$

Combining equations (3.17) and (3.18), we arrive at

$$N_p \sim d^3. \quad (3.21)$$

Therefore, there are  $N_p$  transitions over the volume of the quantum dot and for every transition the oscillator strength is proportional to  $d^{-\beta}$  (eq.3.18), so the total oscillator strength over the volume is proportional to  $N_p d^{-\beta}$ . i.e.,  $\sum_l f_{hl}(\omega_{hl}) = N_p d^{-\beta}$ . So equation (3.17) is reduced to

$$\frac{1}{\tau_{hl}} \sim \frac{\pi e^2 A^2 \omega_{hl} \cos^2 \theta}{mc^2} d^{3-\beta}. \quad (3.22)$$

Taking an arbitrary proportionality  $\eta$  constant which can be determined by considering different properties of the quantum dots, equation (3.22), can be rewritten as:

$$\frac{1}{\tau_{hl}} = \eta \frac{\pi e^2 A^2 \omega_{hl} \cos^2 \theta}{mc^2} d^{3-\beta} \quad (3.23)$$

One can consider all other parameters as a constant except the size of the nc-Si d, it is possible to write the equation (3.23) as:

$$\frac{1}{\tau_{hl}} = \frac{\Theta}{d^{\beta-3}} \quad (3.24)$$

Where  $\Theta = \eta \frac{\pi e^2 A^2 \omega_{hl} \cos^2 \theta}{mc^2}$  which is a parameter that can be determined by studying electronic states; intensity of the incident light and the dielectric function of the amorphous matrix of the nanocrystallinities.

## CHAPTER 4

### Results and Discussion

In this chapter, we will present the result obtained in chapter 3 and discuss the size dependence of the radiative recombination rate we obtained in equation (3.24).

In order to obtain an insight of the effects of size on the PL spectral profile in nc-Si, we use a model as in figure 3.2. The PL emission in visible range is observed when optical transitions between HOMO-LUMO gaps are induced. The photoexcitation is due to the illumination of light, and the photoemission occurs when the photocarriers (electrons and holes) recombine. The electron-hole recombination time (life time of exciton) is strongly dependent on the particle size. The radiative transition in nc-Si may be with or without phonon mediation depending upon the crystallites size. The power exponent of the oscillator strength is larger for the zero phonon assisted case. The Phonon participation decreases as the size of nc-Si decreases, because the band gap changed from indirect to direct due to QCE.

The radiative recombination rate is the most important property in connection with the photoemission efficiency. If the radiative recombination rate is relatively high, a pair comprised an excited electron and hole can recombine via radiative

emission process. If the radiative recombination rate is low, on the other hand, non-radiative recombination events degrade the performance of light emission.

The radiative recombination rate in nc-Si may be with or without phonon mediated depending upon the crystallites size and the nature of the nc-Si (presence of impurity states). As the crystallite size decreases there is no phonon mediation because of the QCE. The QCE changes the energy level spectrum in the bulk material into a discrete level structure namely the sub-band structure. This leads to the enhancement of the oscillator strength of the exciton through increased spatial overlap of between the electron and holes. The strong spatial confinement in the nc-Si implies that for the excitons created in the nc-Si, there is an increase in the radiative recombination rate of the radiative nc-Si. As a result, the quantum efficiency of the system increases. On the other hand non-radiative recombination in the non-radiative nc-Si decreases and the quantum efficiency of this process goes to zero.

We calculate the radiative recombination rate in equation (3.24). Our result shows that the radiative recombination rate ( $\tau^{-1}$ ) depend on the size of crystallites as. Since the power exponent of the oscillator strength is greater than 3 as obtained experimentally by Ranjan and et.al, our calculation shows that increases as the size of the crystallite deceases.

As seen in the previous studies [16], that the PL of nc-si can be readily ascribed to the QCE, the PL being depend on the size of the particles following the law  $E = 1.17 + \frac{3.73}{d^{1.39}}$  [28]. Where E is the energy of the emitted photon and d is

diameter of the particle. According to this experimental result the photon energy emitted increases as the size of the nc-Si decreases. Our work is in conformity with this result.

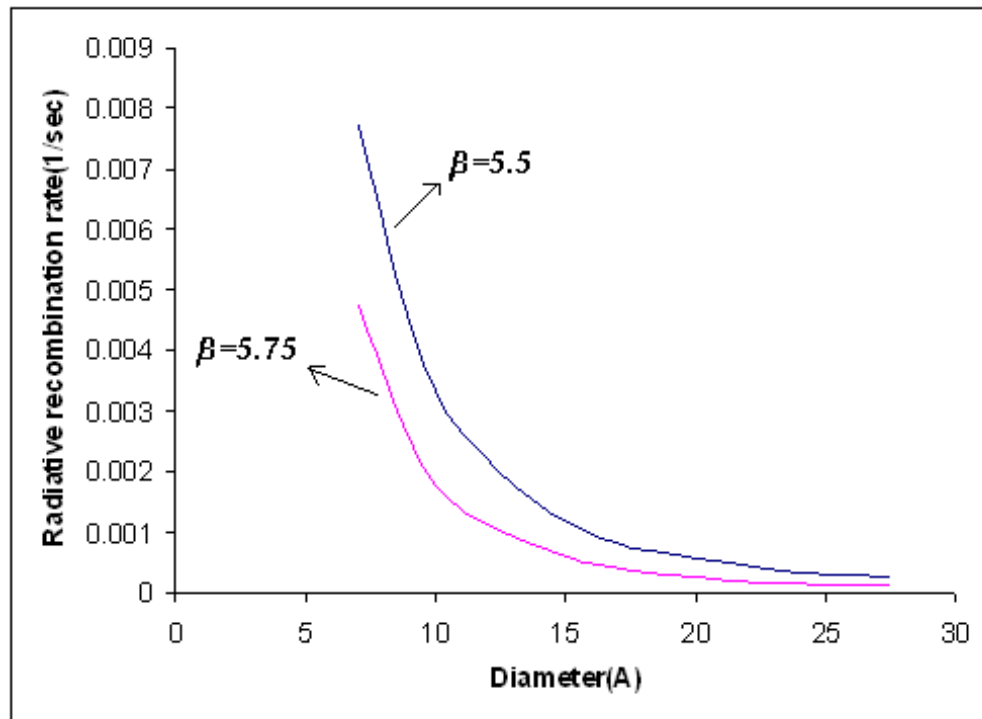
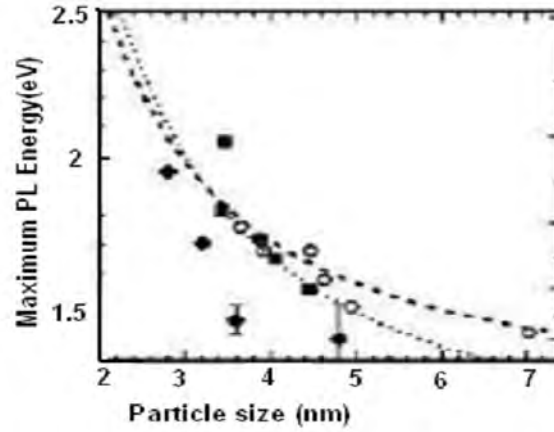


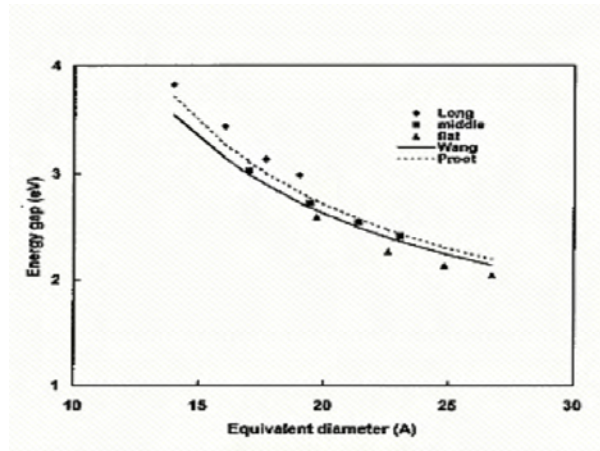
Figure 4.1. The radiative recombination rate as a function of the size of the nc-Si for two values of ( $\beta = 5.5$ ) and ( $\beta = 5.75$ )

Figure 4.1 verifies that for silicon quantum dots having the same properties, the radiative recombination rate increases as the size of the dot decreases. This shows that there exists a strong PL from lower sized nc-Si particles. Recent observation

of PL from nc-Si particles by Calcott and et al [29] shows that the PL energy increases as the size of the particle decreases, as shown in the fig. 4.2. Similarly, in fig. 4.3 we can see that the energy gap between the HOMO and LUMO state increases as the size of the Qds reduces. The increase of the gap energy refers that the photocarriers during optical transitions at least gains energy in the order of the energy gap, so as they can emit light in visible spectrum. Our result is in good agreement with these results.



*Fig.4.2. PL peak energy as a function of particle size (adapted from ref. [29])*



*Fig.4.3 The energy versus equivalent diameter. (adapted from ref [29].)*

## CHAPTER 5

### Summary and Conclusions

In this work we have presented the effect of radiative recombination rate on the PL of nc-Si using the quantum confinement model. The role of quantum confinement model is to treat the nc-Si as the atomic like structure. The model enables us to observe clearly the PL from nc-Si with out surface pasivation. Even if the PL from nc-Si can be enhanced by pasivating the surface with hydrogen or oxygen, in this work we studied the PL of pure nc-Si by calculating the radiative recombination rate.

The pseudopotential method discussed in chapter two gives an overview of the methods used to study the size dependent properties of semiconductor nanocrystal. It is a simple approach to understand the band gap variation of nanocrystal with size and provides a very good description of experimental results.

The wavefunction we use for the HOMO-LUMO state consistes of components of the bulk states in the Brouillon zone, so it is convenient for the analysis of the transition property. Thus our method is suitable for studying the strength of PL caused by the QCE.

P-Si and other systems containing nc-Si have been extensively studied experimentally as well as theoretically. The combination of experimental and theoretical

results enables us to develop a consistent picture of nc-si luminescence. The strong PL of nc-Si is due to exciton confinement energy, the type of recombination process (radiative or non-radiative) and the optical transition oscillator strength (which is inversely proportional to the exciton life time). All these quantities can be traced continuously and smoothly from the bulk silicon PL (infrared spectrum) to the visible spectrum.

Our result shows that the decrease in the size of the nc-Si decreases the exciton life time due to QCE giving strong PL. This is in good agreement with experimental results for P-Si [29].

In conclusion, our work presents a new approach for the PL mechanism of nc-Si. Our theoretical result confirms that low dimensional crystallites manifest strong PL. For the future, using this approach it is possible to study effects of surface pasivation on PL of nc-Si and other related issues. So it is open for further studies.

## References

- [1] D.L. Hareme, J.H. Comfort, J.D.Cressler, E.F.Crabe, J, Y.C. Sun, B.S.Meyerson, and T.Tice, I.E.E.E Trans, Electrton Device, 42,455(1995)
- [2] J.R. Long, M.A.Copeland, S.J. Kovacic, D.S.Malhi, D.L.Hareme, and J.H.wuorinen, 1996 IEEE, ISSCC, Digest of Technical Papers, (San Francisco.CA) ,423, pp.80
- [3] S.K.Ghoshal, K.P. Jain, and R. J. Elliott, Journal of Metastable and Nanocrystalline Materials 23 (2005)
- [4] P.Bettotti, M Cazzanelli, L Dal Negro, B Danese, Z Gaburro, C J Oton, G. Vijaya Prakash and L. Pavesi, J. Phys.: Condens. Matter 14, 8253 (2002)
- [5] C.R.Martin,D.T.Mitchell, Anal. Chem.322A, (1998)
- [6] D.L.Feldheim, C.D.Keating, Chem.soc.Rev.27, 1, (1998)
- [7] S. Sun, C.B. Murray J.Appl.Phys.85, 4325(1999)
- [8] J.Linoros: Silicon Based Microphotonics: From Basis to Application, Ed by O.Bisi, S.U.Camnisano, L.Pavesi, F.Privo. (IOS press, Amsterdam (1999)
- [9] O.Bisis, S.Ossicini and L.Pavesi. Surface science reports 264, 1-126(2000)
- [10] S.K.Ghoshal,Asian Journal of Spectroscopy 7 (2003)
- [11] L.Pavesi and Guardini, Brazilian Journal of Physics 26, No-1(1996)
- [12] A. A. Guzelian, U. Banin, A. V. Kadavanich, X. Peng, and A. P. Alivisatos, Appl. Phys. Lett., 69:10, 1432 (1996)

- [13] P.Harrison, Quantum wells,wires and dots: Theoretical and Computational Physics.John wiley & sons Ltd, Uk (2000)
- [14] C.N.R.Rao, A.Muller and A.K.Cheetham, The Chemistry of Nanomaterials: Synthesis, Properties and Applications. Vol-2 WILEY (2001)
- [15] K.Nisho, J.Koga,T.Yamaguchi and F.Yenezawa, Phys.Rev B 67, 195304 (2003)
- [16] L.T Canham, App Phys.lett.57, No-10, 1046 (1990)
- [17] J.C. Merle, M.Capizi, P.Fiorini and A.Frova. Phys.Rev. B 17, 4821(1978)
- [18] A.L.Erros, M.Rosen, M.Kenwo, M.Nirmal, D.J.norris and M.Bawendi, Phys.rev.B, 54, 4843(1996)
- [19] M.V.Wolkin, J.Jorne, PM.Fauchet, G.Allan,C.Delerue.phys.lett. 83, (1999)
- [20] N.Tessler, V. Medvedev, M. Kazes, S.-H. Kan, and U. Banin, "Efficient Near-Infrared Polymer Nanocrystal Light-Emitting Diodes," Science, 295, 1506 (2002), (Manuscript approved June 2005)
- [21] Lei Lin,C.S. Jayanthi and S,Y.Wng J.Appl. Phys, 90, 4143 (2001)
- [22] S.V. Nair,L.M.Ramaniah.,K.C.Rusrogi, Phys.B,45, 5969(1992)
- [23] J.R. Chelikowsky and M.L. Cohen, Phys Rev. B, 14, 556 (1976).
- [24] D.J. Chadi and M.L. Cohen, Phys. Stat. Sol. (b), 68, 405 (1975).
- [25] G.G.Qin and Y.Q.Jia,Solid state Communication, 86, 559 (1993)
- [26] V.Ranjan,Vijay A.Singh ,George C.John.Phys.Rev.B 58 ,1158-1161(1998)
- [27] M.S.Hybertsen,Phys.Rev.Lett.72.1514(1994)
- [28] C.Delerue, G.Allan, and M. Lannoo, Phys Rev.B 48, 11024(1993)
- [29] P.D.J.Calcott, K.J.Nash, L.T.Canham, M.J.Kane and D.Brumhead, J.Phys.C:Solid State Physics.5L 91(1993).

- [30] Jian-Bai Xia and K W Cheah *J. Phys.: Condens. Matter*, 9, 9853 (1997)  
Printed in the UK{ref 21}

## DECLARATION

I here by declare that this thesis has been presented with the help of my advisor as well as my instructor. All sources of material used for the thesis have been duly acknowledged.

**Name: Gezahegn Assefa**

**Signature: .....**

This thesis has been submitted for the examination with my approval as university advisor.

**Name: Dr. S. K. Ghoshal**

**Signature: .....**

Addis Ababa University  
Department of Physics  
March, 2007